

DISSERTATION ON
***NEUTRON INDUCED REACTION DYNAMICS, USING
DYNAMICAL CLUSTER DECAY MODEL***

SUBMITTED TO



THAPAR UNIVERSITY
(DEEMED TO BE UNIVERSITY UNDER SECTION 3 OF THE UGC ACT, 1956)

BY :-
KOMAL GOYAL
300904020
M.SC. PHYSICS(2009-2011)
THAPAR UNIVERSITY
PATIALA(147004)
INDIA

IN JULY 2011

UNDER THE SUPERVISION OF:-
DR. MANOJ KUMAR SHARMA
ASSOCIATE PROFESSOR
SPMS
THAPAR UNIVERSITY
PATIALA(147004)
INDIA

DEDICATED TO.....

ALMIGHTY GOD
AND
MY FAMILY

CERTIFICATE


It is certified that Komal Goyal (Regn.No.300904020) has completed her M.Sc. thesis on “Neutron Induced Reaction Dynamics, Using Dynamical Cluster Decay Model” under my supervision during the year 2010-2011. She hasn't provided the same material for the credit towards any other degree at Thapar University, Patiala or any other university.


SUPERVISOR:

Dr. Manoj Kumar Sharma
Associate Professor
SPMS
Thapar University
Patiala(147001)
India


Dr. O.P. Pandey
Prof. and Head
SPMS
Thapar University
Patiala(147001)
India

COUNTERSIGNED BY:


Dr. S.K. Mohapatra
Dean of Academic Affairs
Thapar University
Patiala(147001)
India

ACKNOWLEDGEMENT

I sincerely thank to Dr. Manoj Kumar Sharma for his extreme support and supervision during my thesis. He was always there when I needed his guidance and he guided me time to time to make my thesis a success.

I thank Dr. O.P. Pandey for giving M.Sc. students an opportunity like this in which they get a chance to enhance their research capabilities.

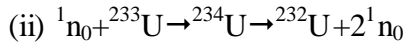
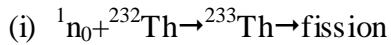
I would also like to thank Ms. Gurvinder Kaur for her timely help and support. She always managed time for me from her schedule and guided me a lot during my project.

I specially thank to my parents for everything they gave to me. I thank them for giving me such a wonderful life. Nothing would have been possible without their blessings.

Kamal Goyal

ABSTRACT

Neutron induced reaction dynamics have been studied using Dynamical Cluster Decay Model (DCM). The DCM based fission as well as neutron cross-sections find nice comparison with experimental data. It may be noted that DCM has been extensively applied for understanding the decay mechanism of nuclear systems formed in heavy ion reactions and its validity is checked in reference to neutron induced reactions for the first time here. The following reactions are worked upon over a wide range of incident energies.



The work presented in this dissertation carries three chapters.

CHAPTER 1

Chapter 1 consists of basics and overview of Accelerator Driven System (ADS). The utility of neutron induced reactions in reference to ADS and nuclear energy etc. is discussed in brief.

CHAPTER 2

Chapter 2 consists of the description of Dynamical Decay Cluster Model (DCM). It gives the description of various potentials used in DCM along with other parameters of the model. The deformation effects of nuclear systems are included in the framework of DCM.

CHAPTER 3

The details of DCM based calculations on ${}^1_0n + {}^{232}\text{Th} \rightarrow {}^{233}\text{Th} \rightarrow \text{fission}$ and ${}^1_0n + {}^{233}\text{U} \rightarrow {}^{234}\text{U} \rightarrow {}^{232}\text{U} + 2{}^1_0n$ reactions are discussed in chapter 3.

CONTENTS

CERTIFICATE.....	3
ACKNOWLEDGEMENT.....	4
ABSTRACT.....	5
LIST OF FIGURES.....	7
<u>CHAPTER-1</u>	
1.1 INTRODUCTION	9
1.2 HISTORY OF ADS	10
1.3 TRANSMUTATION PROCEDURE.....	11
1.4 MAJOR COMPONENTS OF ACCELERATOR DRIVEN SYSTEMS	11
1.5 PICTORIAL VIEW OF ADS	13
1.6 ACCELERATOR DRIVEN TRANSMUTATION PROCESS	14
1.7 BASIC OVERVIEW OF ADS	15
1.8 COMPONENTS OF NUCLEAR WASTE	16
1.9 MAJOR PROBLEMS LINKED WITH CONVENTIONAL THERMAL NUCLEAR REACTORS	16
1.10 APPROACH TO ADS IN INDIA.....	18
1.11 NEUTRON INDUCED REACTION DYNAMICS.....	18
1.12 REFERENCES.....	20
<u>CHAPTER-2</u>	
2.1 INTRODUCTION.....	22
2.2 THE DYNAMICAL CLUSTER DECAY MODEL (DCM) FOR HOT AND ROTATING COMPOUND NUCLEUS	22
2.3 THE FRAGMENTATION POTENTIAL	26
2.4 SOLUTION OF SCHRODINGER EQUATION AND FRAGMENTS PREFORMATION PROBABILITY P_0	28
2.6 PENETRATION PROBABILITY P	29
2.7 REFERENCES	30
<u>CHAPTER-3</u>	
3.1 FISSION OF $^{232}\text{THORIUM}$	33
3.2 U-233(n,2n) CROSS-SECTIONS.....	38
3.3 SUMMARY	41
3.3 REFERENCES	42

LIST OF FIGURES

CHAPTER-1

FIG:1.1 PICTORIAL VIEW OF ADS

FIG:1.2 ENERGY SPECTRUM OF SPALLATION NEUTRONS PRODUCED BY A 1 GEV PROTON BEAM.

FIG:1.3 SCHEMATIC VIEW OF ACCELERATOR DRIVEN SYSTEM.

FIG:1.4 TIME EVOLUTION OF THE POTENTIAL RADIO-TOXICITY(RELATIVE TO URANIUM ORE) OF THE TWO MAIN COMPONENTS OF NUCLEAR WASTE.

CHAPTER-2

FIG:2.1 SCATTERING PLOT OF ${}^1_0n + {}^{232}_{90}\text{Th} \rightarrow {}^{233}_{90}\text{Th}$

CHAPTER-3

FIG:3.1 FRAGMENTATION POTENTIAL OF ${}^1_0n \rightarrow {}^{232}\text{Th} \rightarrow {}^{233}\text{Th} \rightarrow A_1 + A_2$ AT $E_{\text{CM}}=33.8\text{MeV}$ AT $\ell = 0$ AND $\ell_{\text{MAX}}=138$

FIG:3.2 FRAGMENTATION POTENTIAL OF ${}^1_0n + {}^{232}\text{Th} \rightarrow {}^{233}\text{Th} \rightarrow A_1 + A_2$ FOR $E_{\text{CM}} = 33.8\text{MeV}, 45.61\text{MeV}, 59.44\text{MeV}$ AT ℓ_{MAX} VALUES.

FIG:3.3 PREFORMATION PROBABILITY OF FRAGMENTS IN FISSION OF ${}^{233}\text{Th}$ IN NEUTRON INDUCED REACTION AT $E_{\text{CM}}=33.8\text{MeV}$ BY DCM.

FIG:3.4 PREFORMATION PROBABILITY OF FRAGMENTS IN FISSION OF ${}^{233}\text{Th}$ IN NEUTRON INDUCED REACTION AT $E_{\text{CM}}=45.61\text{MeV}$ BY DCM

FIG:3.5 PREFORMATION PROBABILITY OF FRAGMENTS IN FISSION OF ${}^{233}\text{Th}$ IN NEUTRON INDUCED REACTION AT $E_{\text{CM}}=59.44\text{MeV}$ BY DCM

FIG:3.6 PENETRABILITY AS A FUNCTION OF MASS FRAGMENTS A_2 AT $E_{\text{CM}}=33.8\text{MeV}$

FIG:3.7 $(n,2n)$ CROSS-SECTIONS OF ${}^{233}\text{U}$ NUCLEUS

FIG:3.8 DCM BASED FISSION CROSS-SECTIONS COMPARED WITH EXPERIMENT

FIG:3.9 NECK LENGTH PARAMETER AS A FUNCTION OF E_{CM}

CHAPTER-1
BASICS OF ADS

1.1 INTRODUCTION:-

Today, the world is facing an extremely difficult challenge, that of producing sufficient energy to sustain economic growth without affecting the ecological equilibrium of the planet. If the whole of the Earth's population carries out the massive use of fossil fuels, the entire planet would surely be in uncontrollable situation a large number of options have been worked out to meet this evergrowing demand of energy, but still we are not in very happy situation.

Out of the available options an acceptable solution is the essential requirement of today. And the keyrole for this requirement would be played by Nuclear Energy. The real question facing scientists today is: Is it possible to mould nuclear energy production in such a way as to make it more acceptable to society? There have been many technological improvements, mainly with the purpose of improving safety.

Nuclear power production can benefit from the development of more comprehensive alternatives for dealing with long-term radioactive waste. One such alternative is an accelerator-driven subcritical reactor (ADSR) which has been proposed for both the energy production and for burning radioactive waste. Criticality concerns, decay heat management and radioactive waste handling are perceived as the primary, unsatisfactorily resolved technological problems of nuclear reactors. They all originate from very specific features of a fission phenomenon: self-sustained chain reaction in fissile materials, very strong radioactivity of fission products and very long half-life of some of the radioactive fission and activation products. In other words if we could understand the fission process in complete respect then all related issues can be handled simultaneously.

Role of accelerated neutrons:- The spent fuel contains several elements which are resilient to further burning in a nuclear reactor. Therefore, full fission + transmutation cannot be done in an ordinary reactor (using thermal neutrons). In order to eliminate them more efficiently, fast neutrons are necessary. Very fast neutrons are produced by protons accelerated to a medium energy ($\sim 1\text{GeV}$) by a dedicated, compact, high-current accelerator. This device (called Accelerator-Driven System, ADS), is:

1. non critical, since the process rate is fully controlled by the current of the accelerator,
2. preferable to a fast breeder reactor, for higher safety, flexibility and efficiency.

Accelerator-driven transmutation systems, which operate in a subcritical mode and stay subcritical, regardless of the beam being on or off, can in principle address the safety issues associated with criticality. They also provide substantial flexibility in fuel processing and managing. Accelerator-driven transmutation systems can accept such fuels that would be impossible or difficult to use in critical reactors, and can extend their cycle length ensuring good transmutation performance. Moreover, an advanced subcritical core design can also address some concerns of decay heat management.

A subcritical reactor is a nuclear fission reactor that produces fission without achieving criticality. Instead of a sustaining chain reaction, a subcritical reactor uses additional neutrons from an outside source. The neutron source can be a nuclear fusion machine or a particle accelerator producing neutrons by spallation. Such a device with a reactor coupled to an accelerator is called an Accelerator Driven System (ADS) or ATW (i.e. accelerator driven transmutation of wastes.) which in turn integrate a subcritical reactor core, i.e. a fissile material assembly unable to support a self-sustained chain reaction, with an intense spallation neutron source driven by a powerful particle accelerator. This intense neutron source supports the desired fission reaction rate in a fissile assembly taking advantage of the finite neutron multiplication capabilities of this assembly. The basic goal of ADs is reduction of hazards related to handling and management of radioactive wastes through nuclear transmutation and improvement of operational safety of nuclear power facilities. When coupled with the spallation process, high power accelerators can be used for an effective transmutation[2].

Importance of ADS :- ADS opens new possibilities to design subcritical nuclear power reactors combining transmutation with commercial nuclear energy generation. Development of these transmutation systems requires an extensive research program of interdisciplinary dimension covering nuclear physics, nuclear technology including high intensity, medium energy accelerators and spallation targets, reactor physics, material sciences, nuclear chemistry, radioactive waste treatment technologies etc.

1.2 HISTORY OF ADS:-

Concept of an “Accelerator Driven System”(ADS) in the present state, where safety issues and transmutation of waste play an important role, was developed in the late eighties by

a research group at Brookhaven National Laboratory lead by H. Takahashi and G. Van Tuyle [3]. The first detailed design of a transmutation facility using thermal neutrons was published by C. Bowman's Los Alamos group in 1991 introducing a common name The Accelerator Transmutation of Waste (ATW) [5]. In 1993 a group of CERN scientists led by Carlo Rubbia presented the basic concepts of a so-called "Energy Amplifier", a sub-critical nuclear system based on U-Th cycle, fed by a high intensity proton accelerator having the purpose to produce energy with very small amount of Minor Actinide (MA) and Long-Lived Fission Fragment (LLFP) Production.

1.3 TRANSMUTATION PROCEDURE:-

The basic goal of ADS is reduction of hazards related to handling and management of radioactive wastes through nuclear transmutation and improvement of operational safety of nuclear power facilities. As studied earlier most current ADS designs propose a high-intensity proton accelerator with an energy of about 1Gev, directed towards a spallation target made of Thorium that is cooled by liquid lead-bismuth in the core of the reactor. Thus, for each proton interacting in the target, an average of 20 neutrons are created to irradiate the surrounding fuel. Hence, the neutron balance can be regulated in such a way that the reactor would be below criticality if the additional neutrons by the accelerator were not provided. The main advantage provided by this is the inherent safety, whenever the neutron source is turned off, the reaction ceases. Typically, several tens of neutrons will be produced from each proton colliding with the target.[6]. This means that a reasonable beam of protons can produce a large number of neutrons per unit of time.

Nuclear transmutation can be practically induced by any particles or quanta enabled to penetrate nuclei and to interact with nucleons. However, charged particles have to pass through a Coulomb barrier, which requires high energies. The most effective nuclear process that can be used for transmutation of radiotoxic isotopes is neutron absorption. Neutrons are not repelled by nuclei and interaction cross-sections for many transmutation reactions are sufficiently large.

1.4 MAJOR COMPONENTS OF ACCELERATOR DRIVEN SYSTEMS:-

Due to their inherent safety features and waste transmutation potential, accelerator driven subcritical reactors are the subject of research and development in many countries around the world. The ADSR consists of three parts: the accelerator, spallation neutron target and sub-

critical reactor core, explained below :-

1.4.1 ACCELERATOR

Linear or cyclotron accelerators [2] have been proposed for ADS. The optimal parameters of the accelerator are relatively easy to estimate from a nuclear point of view: proton energy should be around 1 – 1.5 GeV (as in Fig. 1– there is no significant gain in number of neutrons per proton energy over 1 GeV) and proton current would depend on desired beam power, which for a demonstration facility would be in the limit of 4–10 MW, corresponding to 5 – 10 mA of the proton current.

Two most powerful accelerators today, represent both accelerators types: LINAC at Los Alamos National Laboratory, running at 800 MeV and 1 – 1.5 mA proton beam, and cyclotron at Paul Scherer Institute, having a 1.8 mA proton beam with 590 MeV energy.

Intensive research work should focus on the following improvements:-

FOR LINACS FOLLOWING FEATURES ARE OBSERVED:

- Improved reliability and trip-free performance,
- Extensive use of superconductors, high-gradient superconducting rf-cavities,
- Increase of electrical field gradients leading to reducing the size,
- Increase of current and possibly beam splitting/sharing to share accelerators in development stage;

FOR CYCLOTRONS FOLLOWING FEATURES ARE OBSERVED:

- Improved reliability and trip-free performance,
- Increase of beam current - novel concepts overcoming space charge difficulties.
- Cost reduction through compactness and robust constructions.

1.4.2 TARGET

The spallation target is at the heart of any accelerator driven system. Few different technical solutions have been envisaged for an ATW spallation target. A solid tungsten target clad in stainless steel and cooled by sodium and a liquid metal target, in which target fluid is also used as the primary cooling loop have been so far presented as the most promising options. The solid tungsten target is less attractive than a liquid metal target; e.g. a liquid Lead-Bismuth eutectic (LBE). Because the ADSR is operated in a subcritical state, the target system has to provide the neutrons needed to sustain fission. These are generated by the spallation process resulting from

high energy protons impacting the spallation target installed at the centre of the core. Therefore the target materials must have high neutron production efficiency. One of the best candidate target material is lead or a lead/bismuth eutectic. The advantages of LBE are chemical inertia, high boiling temperature, relatively low melting temperature (123.5°C), good heat conductivity and no immediate volume expansion upon solidification.

1.4.3. SUB-CRITICAL CORE COOLANT/FUEL SYSTEM:-

Transmutation efficiency and the system performance depend very strongly on the choice of coolant and fuel types. Different conceptual designs have been proposed for the coolant/fuel systems. For an effective transmutation, ATW system requires advanced fuel like metallic, Uranium free-fuel, blend of actinides and Zirconium. This metallic fuel provides the high rates of heat transfer required. Use of a metal fuel makes pyrometallurgical processing attractive for recovery and recycle of the discharged ATW fuel.

1.5 PICTORIAL VIEW OF ADS:-

Pictorial view of ADS is same as that of a conventional thermal nuclear reactor. However major effort must be put to the design of accelerator, beam window spallation target and fuel rods. An ADS works in subcritical condition and its operation is linked to the operation of the accelerator attached to it which provides high energy ion beam to produce spallation neutrons. The ADS remains operational as long as the accelerator functions. The pictorial view of ADS is shown below in fig. 1.1:-

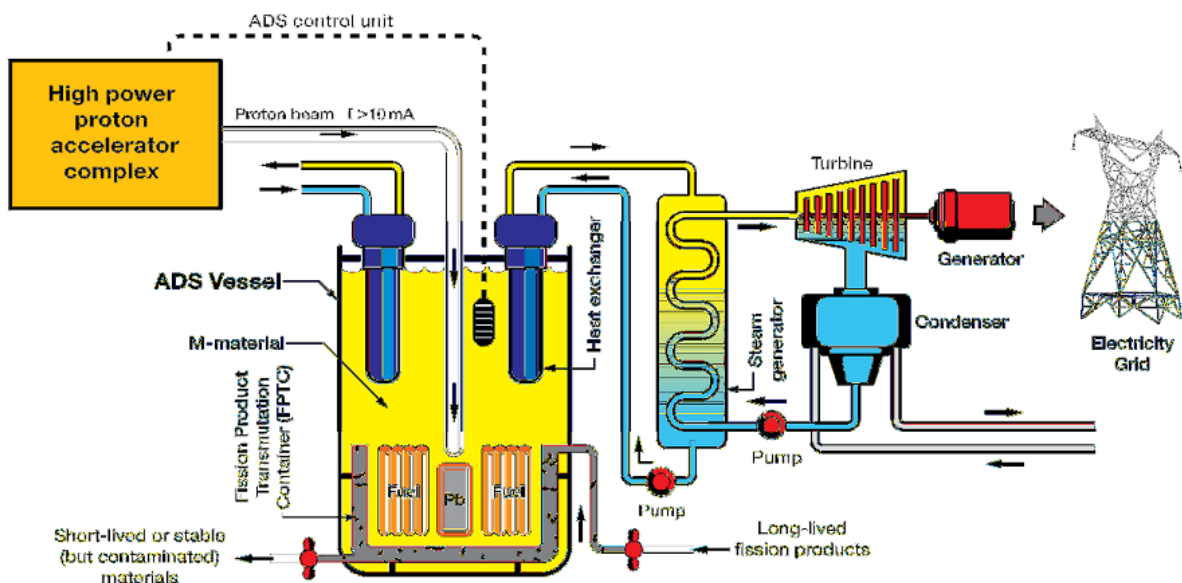


Fig1.1: Pictorial view of ADS

1.6 ACCELERATOR DRIVEN TRANSMUTATION PROCESS:-

When a particle beam (in most designs - protons) from accelerator hits a beam target of heavy elements, large quantities of neutrons and charged particles are obtained, largely through spallation of the atomic nuclei in the target. Most of the charged particles are slowed down and stopped inside the target or in its vicinity as an effect of Coulomb interaction, while the neutrons easily penetrate the target and surrounding subcritical core. If the spallation target is placed in the centre of a subcritical core, the latter can act as a neutron multiplier. This is due to the fact that losses of neutrons can be compensated for through the supply of new neutrons from the spallation target. Through the fissions that occur in the core during neutron multiplication, more energy can be generated than is consumed to produce the accelerator beam. The external neutrons supplied by spallation target sustain a constant power of the system and play the same role as delayed neutrons in critical reactors. This results in another type of “self-sustaining” system, in which delayed neutrons are replaced by the spallation neutrons. Consequently, multiplication coefficient k_{eff} may have values much below 1. That is this system is called subcritical. The criticality of a nuclear assembly is determined by effective neutron multiplication coefficient k_{eff} which is defined as:-

$$k_{eff} = \frac{\text{Number of fissions in any one generation}}{\text{Number of fissions in immediately preceding generation}}$$

The neutrons emerging from both the target and the fuel in the subcritical core originally have high energies varying from a “usual” fission spectrum energies up to an energy of incident protons, as shown in fig 1.2 below:-

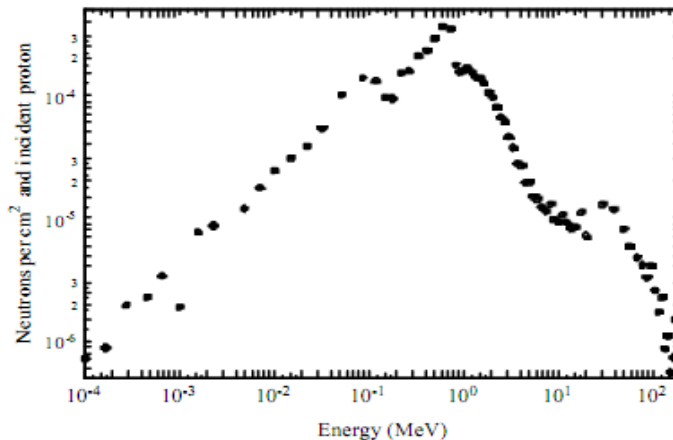


Fig1.2:-Energy spectrum of spallation neutrons produced by a 1 GeV proton beam.[9]

By introducing a moderator, the neutron energy can be reduced (neutrons can be slowed down) in the same way as in a thermal reactor. The advantage of this is that most reaction cross-sections are greater at low neutron energies than at high energies. Conventional moderators - water and graphite - normally require encapsulated solid fuel and are therefore less suitable as moderators in ADS, mainly due to the large gradients in power density. In subcritical systems power density varies in space as exponential function not as cosine or Bessel functions like in critical systems. It results with high power densities around the spallation target and low power on peripheries. Consequently, nuclear fuel in a liquid form is required, e.g. molten salts, where actinides are dissolved in different types of fluoride salts.

Using fast neutron spectrum it is easier to design a suitable subcritical core for ATW than for a critical fast reactor, since the spallation source can deliver neutron flux of very high intensity. Also longer neutron free flow path in the fast systems makes the power peaking problem much less severe than in the thermal systems.

A subcritical reactor can be used to destroy heavy isotopes contained in the used fuel from a conventional nuclear reactor, while at the same time producing electricity. The conversion of heat from the core into electricity is more than sufficient to operate the accelerator.

1.7 BASIC OVERVIEW OF ADS:-

The main components of ADS are a high-intensity accelerator delivering a particle beam of 5 to 40 MW power, a transmuter - a sub-critical reactor with spallation source, and chemical reprocessing[7]. A schematic view of ADS is shown below in fig 1.3:-

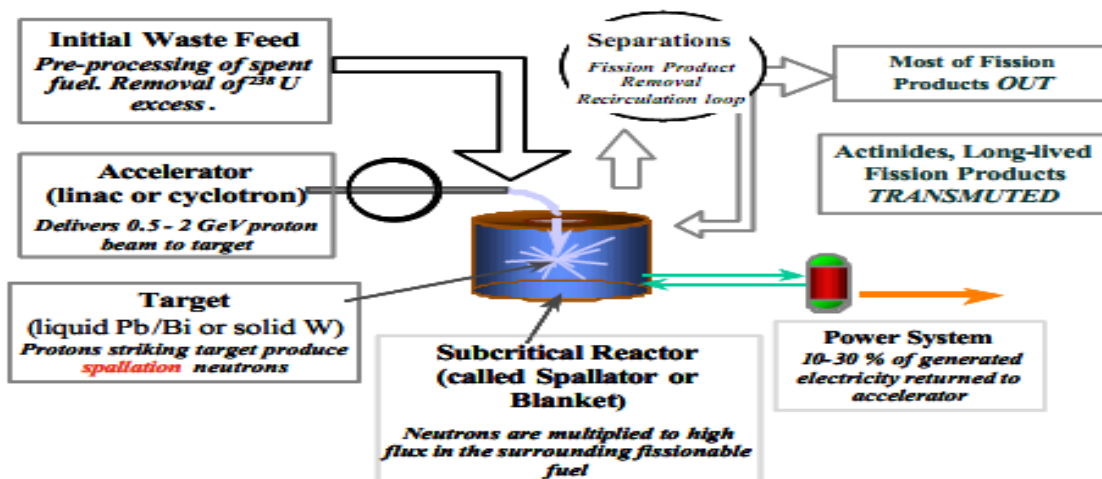


Fig1.3: Schematic view of Accelerator Driven System. [8]

1.8 COMPONENTS OF NUCLEAR WASTE:-

Transuranic elements (TRU) and fission fragments (FF) are the two main components of nuclear waste. TRU, which are produced by neutron capture in the fuel eventually followed by decay, can only be destroyed by fission, while FF can only be destroyed by neutron capture; therefore, different methods will have to be used to eliminate them. Long-term radio-toxicity of waste is dominated by TRU as shown in fig. 1.4 below:-

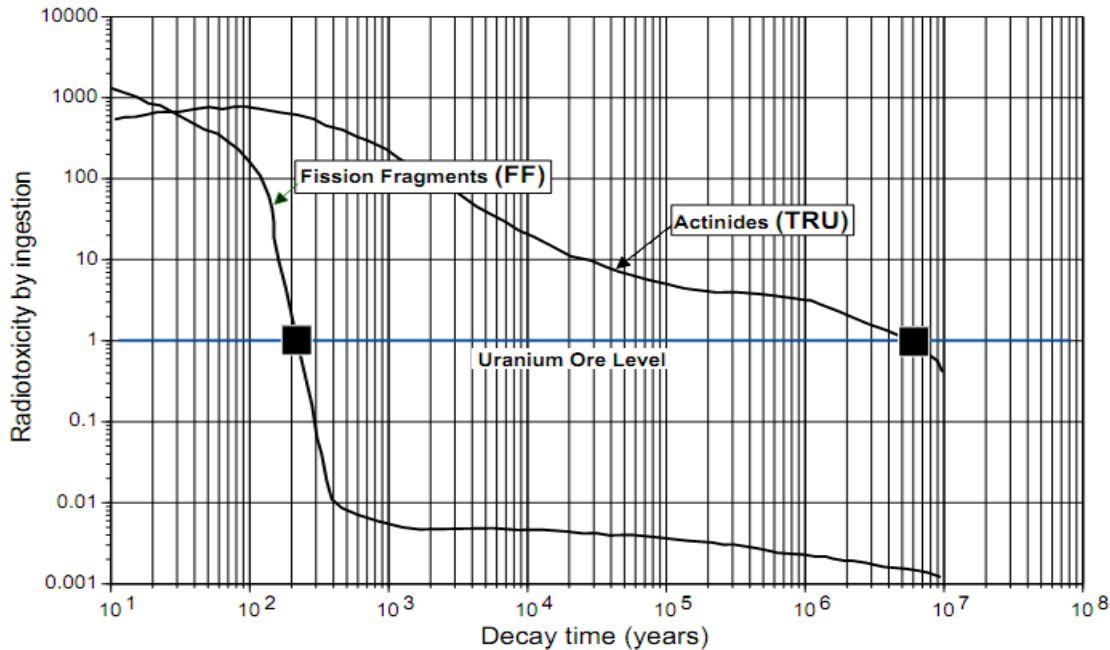


Fig1.4:Time evolution of the potential radio-toxicity(relative to uranium ore)of the two main components of nuclear waste.[10]

1.9 MAJOR PROBLEMS LINKED WITH CONVENTIONAL THERMAL NUCLEAR REACTORS:-

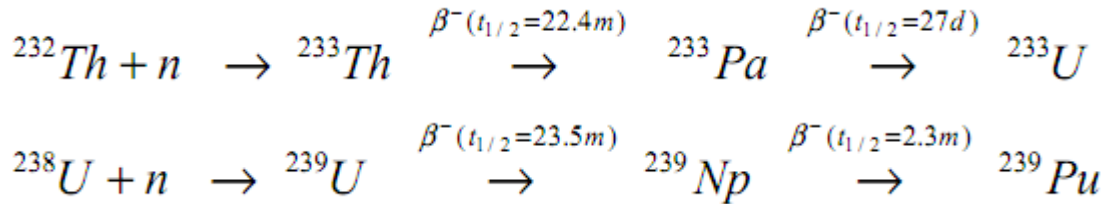
There are four major problems associated with the conventional reactors:

1. Inefficient use of nuclear fuel in the current thermal reactors. Uranium which is a main fuel of reactors has only 1/140 of the abundance of natural uranium. The remaining 99.3% of the uranium is not used in the fuel cycle.
2. Production of long lived nuclear fuel.
3. Safety issues and possibilities of nuclear accidents.
4. Production of fissile material (^{239}Pu), which can be diverted to military applications.

5. To ruleout these three problems one may use ADS and the solution to these problems can be attained in the following manner:-

SOLUTION TO INEFFICIENT USE OF FUEL:

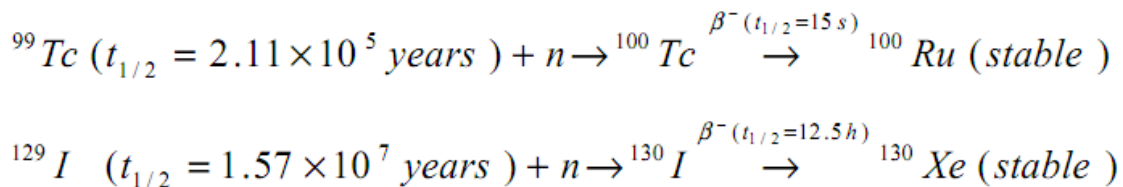
The fuel of ADS is bred from natural thorium or uranium via the following reactions:-



The end product of both reactions is the fissile material that can be used as fuel in ADS.

SOLUTION TO NUCLEAR WASTE PROBLEM:

1. By using more abundant fuel (thorium) very long lived Plutonium and minor actinide radioactive waste will not be produced.
2. ADS is operated in subcritical conditions, therefore excess of neutrons are present in the system. These neutrons can be used to transmute the long lived waste to short lived products via neutron capture process[11,12],for example:



This method of transmutation is not available in conventional nuclear reactors because there are no excess of neutrons. ADS can also transmute the radioactive waste accumulated over 60 years[13].The final nuclear waste of ADS requires only approx. 500 years of storage time (manageable with today's technology) to bring its activity to the level of coal ash[14]. Long lived waste is destroyed by fission process, in such cases energy is also produced[15].

SOLUTION TO NUCLEAR SAFETY ISSUE:

An ADS works in subcritical condition and its operation is linked to the operation of the accelerator attached to it which provides high energy ion beam to produce spallation neutrons. The ADS remains operational as long as the accelerator functions. If proton beam is stopped the

fission reaction stops and hence it never leads to overheating. Moreover an ADS fuelled with Thorium does not contain ^{238}U and therefore will not breed ^{239}Pu which can be diverted to military applications.

1.10 APPROACH TO ADS IN INDIA:-

A roadmap for developing accelerator driven systems (ADS) in India was prepared in 2001. The first phase of the activities under the program began with the commencement of the tenth plan in 2002. The development of a 10 MeV (upgradeable to 20 MeV), 30 mA proton linear accelerator, the setting up of a lead bismuth eutectic (LBE) loop for target and coolant studies and a reactor physics program of developing necessary codes, compiling nuclear data, conceptual design studies of the sub-critical reactor and experimental activities are involved in it. Actual ADS reactor design and development activities are being taken up. Presently, India has a reactor running on HEU fuel viz., APSARA. There is a plan for refurbishing and converting its core to LEU. An advanced high-flux research reactor based on LEU is also planned. Indian interest in ADS has an additional dimension, which is related to the planned utilization of our large Thorium reserves for future nuclear energy generation. Thorium has the added advantage that it produces much less quantities of long lived radioactive actinide wastes as compared to uranium.

1.11 NEUTRON INDUCED REACTION DYNAMICS

The history of fission research based on neutron induced reactions is about seven decades old. Since 1939[16] the neutron induced fission of actinides has been the subject of both fundamental and applied studies. In the past, tremendous effort has been put into studies of low energy actinide fission because of the particular importance of this process for nuclear energy applications. The neutron-induced fission of actinides at low and intermediate energies, i.e., between 1- 200 MeV is still an active field. It is motivated by nuclear data needs for feasibility studies of emerging nuclear systems dedicated to the generation of intense radioactive ion beams, incineration of nuclear waste, isotope production, etc. Nevertheless, after many years of research, neutron-induced fission of actinides remains an intriguing subject of studies in nuclear physics particularly because of its immense application in nuclear reactors for production of nuclear reactors for production of nuclear energy and the understanding of other related aspects.

A number of theoretical models have been proposed at different times to quantitatively predict fragment-mass yields. It is important to note that modelling of low and

intermediate energy neutron-induced fission become complicated because of processes like preequilibrium particle emission and neutron evaporation etc. As a result, a number of nuclides, each with its own fission characteristics, will contribute to the experimental fission observables which further suggests that a model of fragment formation should be embedded in a proper nuclear reaction code which takes care of prefission particle emission.

In neutron reactions the formation of compound nucleus (CN) is quite likely at lower incident energies. Physically this corresponds to a large reflection coefficient in the inside edge of the potential well. Once CN is formed it is assumed that it will decay in a manner that is independent of the mode in which it was formed (complete loss of memory). This is the basic assumption of the model because one can then treat the formation and decay as two separate processes.

The main aim of this work on **“Neutron Induced Reaction Dynamics, Using Dynamical Decay Cluster Model”** is to provide a comprehensive view about ADS and its related aspects in respect to the fact that nuclear energy carries a possible remedy in the issues related to neutron induced reactions. For this purpose, we intend to test the Dynamic Cluster Decay Model, based on well known quantum mechanical fragmentation theory.

It is relevant to mention here that DCM has been used quite extensively to study the heavy ion reactions in the low energy regime. We would like to look out for the possible use of this methodology in the problem related to neutron induced reaction dynamics, which could be of direct relevance to ADS.

The briefs of DCM are given in Chapter 2 and the results are discussed in chapter 3.

1.12 REFERENCES:-

- [1]. W. Gudowski et al., The EC-IABAT Project Final Report, 2000, in print.
- [2]. NEA/OECD Workshop on Utilisation and Reliability of High Power Accelerators, Aix-en-Provence, France, 2-24 November 1999.
- [3]3. G.J. Van Tuyle, H. Takahashi, M. Todosow et al., “The Phoenix Concept. Proposed Transmutation of Long-lived Radioactive Waste to Produce Electric Energy”, BNL 52279, Brookhaven National Laboratory, 1991.
- [4]4. N. Nakamura et al., “Present Status of the OMEGA Program in Japan”, Proc. of the Second OECD/NEA Information Exchange Meeting on Actinide and Fission Product Separation and Transmutation, Argonne, November 11-13, 1992.
- [5]. C.D. Bowman et al., “Nuclear energy generation and waste transmutation using accelerator driven intense thermal neutron source”, LA-UR-91-2601.
- [6].J.Carlsson Msc. Thesis Dep. Of nuclear and reactor physics,Royal inst.of tech.January,1997.
- [7][8][9][10]. W. Gudowski et al., The EC-IABAT Project Final Report, 2000, in print.
- [11].W.Westmeier,R.Brandt,E.J.Langrock,A.N.Sosnin,V.M.Golovatyuk,V.M.Tsoupko Radiochimica,Acta 93(2005)65.
- [12].J.Adam,J.C.Adloff,M.Y.Barabanov,K.M.Hela,R.Odge,P.Vator,J.S.Wan,S.L.Guo,K.K.Dwivedi,B.A.Kulakov,Radiochimica Acta90(2002)431.
- [13].Physics and Safety of Transmutation Systems,A Status Report,Nuclear EnergyAgency,OECD,NEA,No.6090, ISBN 92-64-01082-3,2006.
- [14].C.Rubbia,S.Buono,Y.Kadi,A realistic plutonium fuel,CERN/AT/95-53(ET)1995.
- [15].S.R.HashemiNezhad,R.Brandt,B.A.Kuakov,J.S.Wan, JINR Report,E1-2001-44 A482(2002)537.

CHAPTER-2
DYNAMICAL CLUSTER DECAY
MODEL

2.1 INTRODUCTION

A comprehensive study of various types of emission from the ground state as well as excited states of compound nucleus (CN) formed in low energy reaction is important, as it gives information about the nuclear structure aside the underlying nuclear forces. At low energies and average nuclear force field acts between decaying fragments which in turns ensure possibility of more than one decay path. This average nuclear force field is largely influenced by entrance channel, angular momentum and the temperature consideration along with contribution of deformed and orientation effects. An extensive study of these nuclear properties lead to a better understanding of reaction dynamics. In the present work we intend to apply the Dynamical Cluster Decay Model in the domain of neutron induced reactions. It may be noted that DCM is an established model to understand the decay path of nuclear systems formed in heavy ion reactions at low energies. Although DCM has been extensively applied for investigating decay processes of compound nucleus formed in heavy ion reactions, but so far it has not been applied for neutron induced reaction dynamics. This is first time that DCM is being tested in references to neutron induced reaction dynamics.

This model is a two step model, where the first step is quantum mechanical preformation probability P_0 of the decay products or cluster formed in the mother nuclei and the second step is the penetration of the fragments/ clusters through the interaction barrier.

2.2 The Dynamical Cluster Decay Model (DCM) For Hot and Rotating Compound Nucleus

The dynamical cluster decay model (DCM) [1]-[9] for hot and rotating nuclei (i.e. angular momentum and temperature both not equal to zero) is a reformation of the preformed cluster model of Gupta and collaborators for ground state decay ($\ell = 0, t = 0$) in cluster radioactive (CR) and related phenomena [10]-[18]. Like PCM, DCM is also based upon the dynamical (or quantum mechanical) fragmentation theory of cold phenomena in heavy ion reaction and fission dynamics. In DCM, besides the temperature and angular momentum effects in the decay of excited compound nuclei, the deformation and orientation effect of the decay products are also taken care, especially in the decay of heavy excited CN for which the deformation of the decay

product seems to play significant role. The DCM, worked out in terms of the collective coordinates of mass asymmetry $\eta = \frac{A_1 - A_2}{A_1 + A_2}$ and relative separation R respectively gives

- (i). The nucleon-division (or exchange) between the outgoing fragments, and
- (ii). the transfer of kinetic energy of incident channel (E_{cm}) to internal excitation (total excitation or total kinetic energy, TXE or TKE) of the outgoing channel. It may be noted that the fixed decay point $R = R_a$ (defined later), at which the process is calculated depends upon temperature T as well as on η (i.e. $R(T, \eta)$)

$$E_{CN}^* = E_{c.m.} + Q_{in} = I Q_{out} + TKE(T) + TXE(T) \quad (2.1)$$

The CN excitation E_{CN}^* is related to temperature T (in MeV) and is given by

$$E_{CN}^* = \frac{1}{9} AT^2 - T(Mev) .$$

Using the decoupled approximation to R and η -motions, the DCM define the decay cross section, in terms of partial waves, as [3]-[9] ;

$$k = \sqrt{\frac{(2\mu E_{c.m.})}{\hbar^2}} ; \sigma = \sum_{l=0}^{l_c} \sigma_l = \frac{\pi}{k^2} \sum_{l=0}^{l_c} (2l+1) P_0 P \quad (2.2)$$

Where P_0 , the preformation probability refers to η -motion and P, the penetrability to the R-motion. Here the complex fragments (both light and heavy fragments) are treated as the dynamical collective mass motion of preformed cluster or fragments through the barrier. The structure information of the CN enters the model via preformation probability P_0 (also known as spectroscopic factor) of the fragments given by the solution of stationary Schrödinger equation in η at the fixed $R=R_a$, the first turning point of the penetrability path.

$$\left\{ -\frac{\hbar^2}{2\sqrt{B_{\eta\eta}}} \frac{\partial}{\partial \eta} \frac{1}{\sqrt{B_{\eta\eta}}} \frac{\partial}{\partial \eta} + V_R(\eta, T) \right\} \psi^\nu(\eta) = E^\nu \psi^\nu(\eta) \quad (2.3)$$

with $\nu=0,1,2,3,\dots$ referring to the ground state and excited state solution .

For the decay of the hot compound nucleus, we use the postulate of first turning point

$$R_a = R_t + \Delta R(T) \quad (2.4)$$

Where

$$R_t = R_1 + R_2 \quad (2.5)$$

$\Delta R(T)$ is the neck length parameter that assimilates the neck formation effects. This method is introducing a neck length parameter similar to that used in scission point [19] and saddle point

[20],[21]statistical fission model. The R_i are radius vectors which are also made temperature dependent can be calculated as

$$R_i(\alpha_i) = R_{0i} \left[1 + \sum_{\lambda} \beta_{\lambda i} Y_{\lambda}^{(0)}(\alpha_i) \right] \quad (2.6)$$

With

$$R_{0i}(T) = 1.28 A_i^{1/3} - 0.76 + 0.8 A_i^{-1/3} \times (1 + 0.0007 T^2), \quad (2.7)$$

The corresponding potential $V(R_a)$ acts like an effective Q-value, Q_{eff} , for the decay of the hot CN at temperature T , to two exit-channel fragments observed in g.s. ($T=0$), defined by

$$\begin{aligned} Q_{\text{eff}}(T) &= B(T) - [B_L(T=0) + B_H(T=0)] \\ &= \text{TKE}(T) = V(R_a(T)) \end{aligned} \quad (2.8)$$

with B 's as the respective binding energies.

The above defined decay of a hot CN into two cold ($T=0$) fragments, via Eq.(2.8), could apparently be achieved only by emitting some light particle (s)(LPs), like n , p , α , or γ -rays of energy

By defining $Q_{\text{eff}}(T)$ as in Eq. (2.8), in this model we treat the LP emission at par with the heavy fragments, called intermediate mass fragments (IMFs) emission. Thus, in this model a non-statistical dynamical treatment is attempted for not only the emission of IMFs but also of multiple LPs, understood so-far only as the statistically evaporated particles in a CN emission. It may be reminded here that the statistical model (CN emission) interpretation of IMFs is not as good as it is for the LP production [19–24].

In terms of $Q_{\text{eff}}(T)$, the second turning R_b satisfies

$$V(R_a, l) = V(R_b, l) = Q_{\text{eff}}(T) = \text{TKE}(T). \quad (2.9)$$

with the l -dependence of R_a defined by:

$$V(R_a, l) = Q_{\text{eff}}(T, l=0), \quad (2.10)$$

which means that the R_a , given by Eq. (2.4), is the same for all l -values, and that $V(R_a, l)$ acts like an effective Q-value, $Q_{\text{eff}}(T, l)$, given by the total kinetic energy $\text{TKE}(T)$. Then, using (2.9), $R_b(l)$ is given by the l -dependent scattering potentials, at fixed T as:

$$V(R, T, l) = V_c(Z_i, \beta_{\lambda i}, \theta_i, T) + V_p(A_i, \beta_{\lambda i}, \theta_i, T) + V_i(R, A_i, \beta_{\lambda i}, \theta_i, T) \quad (2.11)$$

which is normalized to the exit channel binding energy $B_L(T) + B_H(T)$. Such a potential is illustrated in Fig 2.1

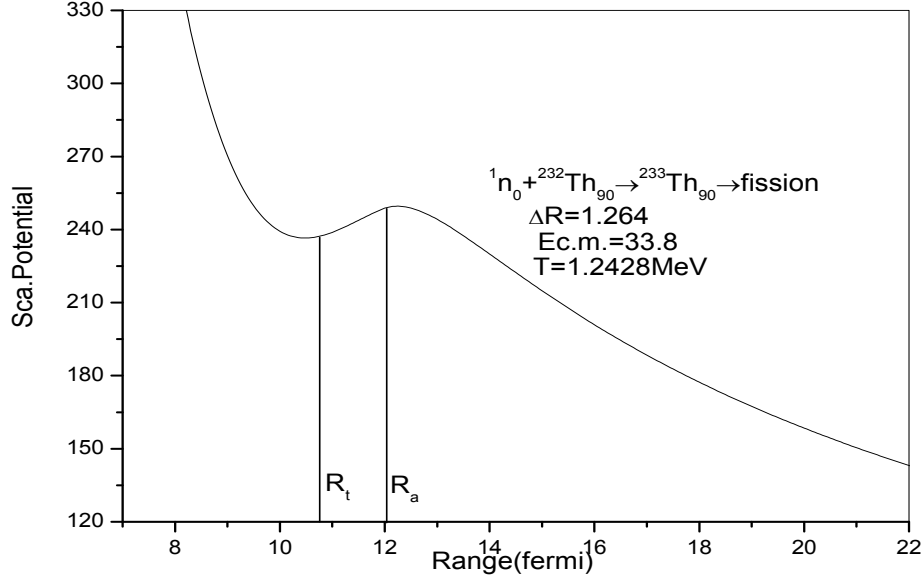


Fig2.1:-Scattering Plot of ${}^{232}\text{Th}_{90} + {}^1_0n \rightarrow {}^{233}\text{Th}_{90}$

The collective fragmentation potential $V(R,\eta,T)$ in Eq. (2.11) is calculated according to the Strutinsky method by using the T-dependent liquid drop model energy V_{LDM} of [25], with its constants at $T=0$ re-fitted [3,4] to give the recent experimental binding energies given by [26], and again refitted [9] to give the recent experimental binding energies[29] and calculate binding energies[34] (only for those nuclides for which experimental data is not available. the “empirical” shell corrections δU are of Ref. [29] (In the Appendix of [3] and Eq. (8) of [4], $a_a=0.5$, instead of unity). Then, including the T-dependence also in Coulomb, nuclear proximity, and l -dependent potential in complete sticking limit of moment of inertia, we get

$$\begin{aligned}
 &V(R, \eta, T) \\
 &= \sum_{i=1}^2 [V_{\text{LDM}}(A_i, Z_i, T) + \sum_{i=1}^2 [\delta U_i] \exp\left(\frac{-T^2}{T_0^2}\right) + V_c(Z_i, \beta_{\lambda_i}, \theta_i, T) + V_p(A_i, \beta_{\lambda_i}, \theta_i, T) \\
 &+ V_l(R, \beta_{\lambda_i}, \theta_i, T) \tag{2.12}
 \end{aligned}$$

where the T-dependent terms V_c , V_p and V_l are defined as follows: The proximity potential for hot deformed nuclei is [33],[34]

$$V_p(A_i, \beta_{\lambda_i}, \theta_i, T) = 4\pi R(T) \gamma b(T) \Phi(s_0(T)) \tag{2.13}$$

and, the Coulomb Potential

$$V_c(Z_i, \beta_{\lambda_i}, \theta_i, T) = \frac{Z_1 Z_2 e^2}{R(T)} + 3Z_1 Z_2 e^2 \sum_{i,i=1,2} \frac{R_i^\lambda(\alpha_i, T)}{(2\lambda+1)R(T)^{\lambda+1}} Y_\lambda^{(0)}(\theta_i) [\beta_{\lambda_i} + \beta_{\lambda_i}^2 Y_\lambda^{(0)}(\theta_i)] \quad (2.14)$$

with the radius vector given by Eq. (2.6) and surface thickness parameter

$$b(T) = 0.99(1 + 0.009T^2). \quad (2.15)$$

The angular momentum potential, (see section 2.3.5)

$$V_l(R, A_i, \beta_{\lambda_i}, \theta_i, T) = \frac{\hbar^2 l(l+1)}{2I_s(T)} \quad (2.16)$$

with the moment-of-inertia,

$$I_s(T) = \mu R^2 + \frac{2}{5} A_1 m R_1^2(\alpha_1, T) + \frac{2}{5} A_2 m R_2^2(\alpha_2, T).$$

Further, in Eq. (2.12), within the Strutinsky renormalization procedure we have defined the binding energy B of a nucleus at temperature T as the sum of liquid drop energy $V_{LDM}(T)$ and shell correction $\delta U(T)$ i.e.

$$B(T) = V_{LDM}(T) + \delta U \exp\left(\frac{-T^2}{T_0^2}\right) \quad (2.17)$$

The T dependent liquid drop part of the binding energy $V_{LDM}(T)$ is from Davidson et al. [25], based on the semi-empirical mass formula of Seeger [36]. For the shell correction δU in Eq. (2.17), since there is no microscopic shell model known that gives the shell corrections for light nuclei, we use the empirical formula of Myers and Swiatecki [35].

The mass parameters $B_{\eta\eta}(\eta)$, representing the kinetic energy part in Eq. (2.3), are the smooth classical hydro-dynamical masses [31].

Finally, the l_c -value in Eq. (2.6) is the critical l -value, in terms of the bombarding energy $E_{c.m.}$, the reduced mass μ and the first turning point R_a of the entrance channel η_{in} , given by

$$l_c = R_a \sqrt{(2\mu[E_{c.m.} - V(R_a, \eta_{in}, l=0)])/\hbar} \quad (2.18)$$

or, alternatively, it could be fixed for the vanishing of fusion barrier of the incoming channel, called l_{fus} , or else the l -value (l_{max}) where the light-particle cross section $\sigma_{LP} \rightarrow 0$. This, however, could also be taken as a variable parameter [20,32].

2.3 The Fragmentation potential $V(\eta)$ The collective potential energy or the fragmentation potential $V(\eta, R)$, appearing in equation (2.8) is calculated as,

$$V(\eta, R) = -\sum_{i=1}^2 B_i(A_i, Z_i, \beta_{\lambda_i}) + V_c(R, Z_i, \beta_{\lambda_i}, \theta_i, \varphi) + V_p(R, A_i, \beta_{\lambda_i}, \theta_i, \varphi) + V_l(R, A_i, \beta_{\lambda_i}, \theta_i, \varphi) \quad (2.19)$$

Here B_i ($i=1,2$) are the binding energies of the two nuclei, available from the experimental data

of Audi-wapstra [33]. Wherever the experimental B's are not available, the theoretical binding energies of Moller et al.[34] are used. Note that the binding energies contain both the macroscopic (liquid drop part) and the microscopic (shell correction part).

The fragmentation potential $V(\eta)$ is calculated at a fixed distance $R=R_1+R_2+\delta R$ or $R=C_1+C_2+\delta C$ fm, with C_i ($i=1,2$) as the süssmann central radii related to the radius vector R_i as $C_i = R_i(1 - b^2/R_i^2)$ with

$$R_i = R_{0i} [1 + \sum_{\lambda} \beta_{\lambda i} Y_{\lambda}^{(0)}(\alpha_i)], \quad (2.20)$$

and

$$R_{0i} = 1.28A_i^{1/3} - 0.76 + 0.8A_i^{-1/3} \quad (2.21)$$

Here $\lambda=2,3,4,\dots$ and α_i is an angle that the radius vector R_i of the colliding nuclei makes with the symmetry axis the diffuseness of the nuclear surface (I.e. the surface thickness) $b = 0.99$ fm. The charges Z_i are fixed by minimizing the potential $V(\eta)$ in the η_Z coordinate at each η value.

For the study of excited systems, where the nuclear temperature effects also come into picture, the fragmentation potential at fixed R is

$$V(\eta, T) = \sum_{i=1}^2 V_{LDM}(A_i, Z_i, T) + \sum_{i=1}^2 \delta U \exp(-T^2/T_0^2) + V_c(Z_i, \beta_{\lambda i}, \theta_i, \varphi, T) + V_p(A_i, \beta_{\lambda i}, \theta_i, \varphi, T) + V_l(A_i, \beta_{\lambda i}, \theta_i, \varphi, T) \quad (2.22)$$

Here, $V_{LDM}(A_i, Z_i, T)$ is the liquid drop part of the binding energy and δU , the shell corrections. Note that the calculation of fragmentation potential involves all the possible decay channels and the number of all such possible decay channels becomes more and more with the increasing mass of the mother nucleus. The nuclear temperature T (in MeV) is related to the excitation energy E_{CN}^* of the compound nucleus, through a semi-empirical statistical relation as:

$$E_{CN}^* = 1/10AT^2 - T \text{ (MeV)} \quad (2.23)$$

The shell corrections δU in Eq. (2.34) are considered to vanish exponentially for $E_{CN}^* \geq 60$ MeV, giving $T_0 = 1.5$ MeV. At higher excitation energies the shell corrections vanish completely and only the liquid drop part of energy is present. The shell corrections play an important role in determining or empirical fitting of nuclear masses, because the nuclear masses calculated by using the smooth liquid drop formula show large deviations with respect to the experimental

masses. It means that in the experimental masses there exist deep minima at specific neutron and/or proton numbers indicating the presence of shell structure, the so-called magic numbers in nuclei. This characteristic behavior cannot be reproduced by the liquid drop part alone, which means that the introduction of microscopic shell correction in the mass formula is essential. Thus, shell corrections accounts for the removal of deviation from the liquid drop calculations (uniform distribution of nucleons), and are defined, within Strutinsky [37] method as

$$\delta U = U - \tilde{U} \quad (2.24)$$

where, $U = \sum_{\nu} E_{\nu} 2n_{\nu}$ is the sum over all occupied single particle states and

$$\tilde{U} = \int_{-\infty}^j E \tilde{g}(E) dE \quad (2.25)$$

is the average energy for uniform distribution. In general, the microscopic shell correction, together with the liquid drop part, gives a proper description of the binding energy of the nucleus. This method, however, does not give a proper description of light mass nuclei. The difficulty is the inadequacy of shell model for very light nuclei. For this reason, the macro-microscopic calculations of Moller et al. [34] are tabulated for $Z \geq 8$ only. For $Z \leq 8$, one could alternatively use the empirical shell correction method of Myers-Swiatecki [38] which again is not very satisfactory for light nuclei ($Z \leq 16$). Gupta and collaborators have modified this empirical method and obtained a better description of the shell corrections for the light as well as heavy mass region, i.e., $1 \leq Z \leq 118$ [4].

2.4 Solution of the Schrödinger Equation and the fragments

Preformation Probability P_0

Once the Hamiltonian Eq. (2.25) is established, the Schrödinger equation in mass fragmentation co-ordinate η can be solved. On solving Eq. (2.26) numerically, $|\psi^{\nu}(\eta)|^2$ gives the probability P_0 of finding the mass fragmentation η at a fixed R on the decay path.

$$P_0(A_2) = |\psi^{\nu}(A_2)|^2 \quad (2.26)$$

For fission studies, like the spontaneous fission and fission through the barrier, the motion in R at the saddle point is adiabatically slow as compared to the η motion. Therefore, the potential is minimized in the neck and deformation coordinates β_1 and β_2 at each R and η values. Starting from the nuclear ground state in spontaneous fission or cluster decay, and to have complete

adiabaticity, only the lowest vibrational state $\nu = 0$ is occupied. Then, the mass (or charge) distribution yield, proportional to the probability $|\psi^{(0)}(\eta)|^2$ or $|\psi^{(0)}(\eta_Z)|^2$ of finding a certain mass (or charge) fragmentation η (or η_Z) at a position R on the decay path, when scaled to, say, mass A_2 of one of the fragments ($d\eta = 2/A$) is given by:

$$Y(A_2) = |\psi_R^{(0)}(A_2)|^2 \frac{2}{A} \sqrt{B_{\eta\eta}(A_2)}. \quad (2.27)$$

However, if the system is excited or we allow interaction between various degrees of freedom, higher values of ν would also contribute. These enter via the excitation of higher vibrational states, and through the temperature dependent potential V and masses B_{ij} . The effect of adding temperature on potential V and masses B_{ij} is to reduce the shell effects in them, resulting finally in the liquid drop potential VLDM and smoothed (averaged) masses B_{ij} for the systems to be very hot. Apparently, cold fission means taking both the potential V and masses B_{ij} with full shell effects included in them and hot fission means using the VLDM and smoothed (averaged) masses B_{ij} . The possible consequence of such excitations are included here by assuming a Boltzmann like occupation of excited states

$$|\psi(\eta)|^2 = \sum_{\nu=0}^{\infty} |\psi^{\nu}(\eta)|^2 \exp\left(-\frac{E_{\eta}^{\nu}}{T}\right) \quad (2.28)$$

Note that we are dealing here with a directly measurable quantity, the mass (or charge) asymmetry, which works dynamically as mass (or charge) transfer coordinate. Thus, the calculated yields $Y(A_i)$ (or $Y(Z_i)$) are directly comparable with experiments. It may be stressed that there is no free parameter in these calculations. The nuclear shape, once minimized in the neck and deformation coordinates β_1 and β_2 at a given R ($=R_{\text{saddle}}$), remains fixed for both the mass and charge distributions of fission or decay fragments.

2.5 Penetration Probability P

Penetrability P measures the capability of fragments nucleus to penetrate the potential barrier generalized during compound nucleus formation.

The penetrability P_i , in terms of its barrier height $V_B^{\ell}(E_{c.m.}, \theta_i)$ and curvature $\hbar\omega_{\ell}(E_{c.m.}, \theta_i)$, is

$$P_i = \left[1 + \exp\left(\frac{2\pi(V_B^{\ell}(E_{c.m.}, \theta_i) - E_{c.m.})}{\hbar\omega_{\ell}(E_{c.m.}, \theta_i)}\right)\right]^{-1} \quad (2.29)$$

2.6 REFERENCES

- [1] R.K. Gupta, M. Balasubramiam, C. Mazzocchi, M. La Commara, and W.Scheid, Phys. Rev. C 65, 024601 (2002).
- [2] M.K. Sharma, R.K. Gupta, and W. Scheid, J. Phys. G 26, L45 (2000).
- [3] R.K. Gupta, R. Kumar, N.K. Dhiman, M. Balasubramiam, W. Scheid, and C.Beck, Phys. Rev. C 68, 014610 (2003).
- [4] M. Balasubramiam, R. Kumar, R.K. Gupta, C. Beck, and W. Scheid, J. Phys.G 29, 2703 (2003): R.K. Gupta, M.K. Sharma and B. Singh, Phys. Rev. C-to be published
- [5] R.K. Gupta, M. Balasubramiam, R. Kumar, D. Singh, and C. Beck, Nucl.Phys. A 738, 479c (2004).
- [6] R.K. Gupta, M. Balasubramiam, R. Kumar, D. Singh, C. Beck, and W.Greiner, Phys. Rev. C 71, 014601 (2005).
- [7] B.B. Singh, M.K. Sharma, R.K. Gupta, and W.Greiner, Int.J. Mod.Phys.E15, 699 (2006)
- [8] R.K. Gupta, M. Balasubramiam, R.Kumar, D.Singh ,S. K. Arun and W.Greiner, J.Phys .G:Nucl.Part. Phys. 32,345(2006)
- [9] B.B. Singh, M.K. Sharma, R.K. Gupta, Phys.Rev. C 77, 054613 (2008)
- [10] R.Gupta, in proceedings of the 5th International Conference on Nuclear Research Mechanics, Varenna, 1988, edited by E. gladioli , (Ricerca Scientifica ed Educazione Permanente ,Milano, 1988),p.416.
- [11] S.S. Malik and R.K.Gupta, Phys.Rev.C 39, 1992(1989)
- [12] R.K.Gupta, W.Scheid, and W.Greiner, J.Phys.G:Nucl. Part. Phys. 17, 1731(1991).
- [13] S. Kumar and R.K.Gupta, Phys.Rev. C 49, 1922(1994).
- [14] R.K.Gupta and W. Greiner Int. J. Mod. Phys. E 3, 335 (1994, Suppl.).
- [15] S. Kumar and R.K.Gupta, Phys. Rev. C 55, 218 (1997).
- [16] R.K. Gupta, in Heavy Elements and Related New Phenomena ,edited by W.Greiner and R.K Gupta (World Scientific Singapore) Vol.II ,p.730
- [17] S.K and R.K Gupta ,DAE nucl.Phys.(Sambalpur)52,365(2007)
- [18] B.B.Singh,S.K Arun, M.K.Sharma , S.Kanwar and Raj K.Gupta ,DAE Nucl.Phys.(Roorkee), Accepted(2008)
- [19] T. Matsuse, C. Beck, R. Nouicer, and D. Mahboub, Phys. Rev. C 55, 1380(1997).

- [20] S.J. Sanders, D.G. Kovar, B.B. Back, C. Beck, D.J. Henderson, R.V.F. Janssens, T.F. Wang, and B.D. Wilkins, *Phys. Rev. C* 40, 2091 (1989t).
- [21] S.J. Sanders, *Phys. Rev. C* 44, 2676 (1991).
- [22] J. Gomez del Campo, R.L. Auble, J.R. Beene, M.L. Halbert, H.J. Kim, A.D'Onofrio, and J.L. Charvet, *Phys. Rev. C* 43, 2689 (1991); *Phys. Rev. Lett.* 61, 290 (1988).
- [23] R.J. Charity, M.A. McMahan, G.J. Wozniak, R.J. McDonald, L. G. Moretto, D.G. Sarantites, L.G. Sobotka, G. Guarino, A. Pantaleo, L. Fiore, A. Gobbi and K.D. Hildenbrand, *Nucl. Phys. A* 483, 371 (1988).
- [24] C. Beck, R. Nouicer, D. Disdier, G. Duchêne, G. de France, R.M. Freeman, F. Haas, A. Hachem, D. Mahboub, V. Rauch, M. Rousseau, S.J. Sanders, and A. Szanto de Toledo, *Phys. Rev. C* 63, 014607 (2001).
- [25] N.J. Davidson, S.S. Hsiao, J. Markram, H.G. Miller, and Y. Tzeng, *Nucl. Phys. A* 570, 61c (1994).
- [26] G. Audi and A.H. Wapstra, *Nucl. Phys. A* 595, 4 (1995).
- [27] G. Audi and A.H. Wapstra and C. Thiboult, *Nucl. Phys. A* 729, 337 (2003)
- [28] P. Moller, J. R. Nix, W. D. Myers, and W. J. Swiatecki, *At. Data Nucl. Data Tables* 59, 185 (1995).
- [29] W. Myers and W.J. Swiatecki, *Nucl. Phys.* 81, 1 (1966).
- [30] P. A. Seeger, *Nucl. Phys.* 25, 1 (1961)
- [31] H. Kroger and W. Scheid, *J. Phys. G* 6, L85 (1980)
- [32] S.J. Sanders, D.G. Kovar, B.B. Back, C. Beck, B.K. Dichter, D. Henderson, R.V.F. Janssens, J.G. Keller, S. Kaufman, T.-F. Wang, B. Wilkins, and F. Videbaek, *Phys. Rev. Lett.* 59, 2856 (1987).
- [33] G. Audi and A.H. Wapstra and C. Thiboult, *Nucl. Phys. A* 729, 337 (2003)
- [34] P. Moller, J. R. Nix, W. D. Myers, and W. J. Swiatecki, *At. Data Nucl. Data Tables* 59, 185 (1995).
- [35] W. Myers and W.J. Swiatecki, *Nucl. Phys.* 81, 1 (1966).
- [36] P. A. Seeger, *Nucl. Phys.* 25, 1 (1961)
- [37] V.M. Strutinsky, *Nucl. Phys. A* 95, 420 (1967).
- [38] J. Gomez del Campo, R.L. Auble, J.R. Beene, M.L. Halbert, H.J. Kim, A.D'Onofrio, and J.L. Charvet, *Phys. Rev. C* 43, 2689 (1991); *Phys. Rev. Lett.* 61, 290 (1988).

CHAPTER-3
CALCULATIONS AND RESULTS

CALCULATIONS AND RESULTS

Reactions in Accelerator Driven systems like conventional nuclear reactors are based on neutron induced reactions. The neutron induced reactions can be broadly classified as fission reactions (n,f) and (n,xn) reactions.

The Dynamic Cluster Decay Model(DCM) has been applied for the first time in the domain of neutron induced reaction dynamics after being quite successful in the heavy ion induced reaction dynamics. It may be noted that DCM has been applied extensively for understanding the decay mechanism of nuclear systems formed in heavy ion reactions at low, intermediate, heavy and super heavy region and it will be of immense interest to see its utility in reference to neutron induced reactions.

3.1 FISSION OF ^{232}Th ($^{232}\text{Th}(n,f)$)

As we know that fission research started in 1939 with the discovery of neutron induced fission of Uranium [1]. From that time onward the neutron induced fission of actinides has been the subject of both fundamental and applied studies. Tremendous efforts has been put into studies of low energy actinide fission because of the particular importance of this process for nuclear energy applications. These days the neutron-induced fission of actinides at intermediate energies is also being investigated. These studies are motivated by nuclear data needs for feasibility studies of emerging nuclear systems dedicated to the generation of intense radioactive ion beams, isotope production and related phenomenon.

The fragment mass distribution is one of the most important characteristics of nuclear fission process. Despite of being such an old concept, an overall understanding of fission process is still not understood completely, particularly with the invent of phenomenon like quasi fission, pre-equilibrium fission, fusion hindrance etc. The concept of potential energy surfaces has been utilized to demonstrate the fission fragment distribution, along with other related aspects like role of nuclear friction, inertia, angular momentum, deformation, orientation and temperature etc. A large number of theoretical models have been

used for qualitative and quantitative description of fission mass yields[2-8]. As mentioned earlier DCM has been very successful in explaining the fragmentation process of nuclear systems formed in heavy ion reactions and now it will be of extreme interest to apply it in the framework of neutron induced reactions.

In this work we are representing the fragment mass yields and fission cross-sections of ^{232}Th at energies from 30 to 60 MeV, calculated with the help of **Dynamical Cluster Decay Model**. The neutron induced fission cross-sections for [$^1_0\text{n} + ^{232}\text{Th} \rightarrow ^{233}\text{Th} \rightarrow \text{fission}$] has been studied at energies $E_{c.m.}=33.8, 45.61$ and 59.44 MeV [1][9]. In reference to this experiment, DCM based calculations are made for above mentioned reaction with one parameter i.e. neck length parameter (ΔR) by including deformation effects upto quadrupole effects i.e. β_2 at optimum orientation criteria.

TABLE 3.1 DCM based neutron induced fission cross-sections compared with experimental data.

S.NO.	Ecm (MeV)	Temp	ΔR (Fermi)	ℓ_{max}	σ_{fission} (DCM) (mb)	$\Sigma_{\text{fission}}(\text{expt.})$ (mb)
1	33.8	1.2428	1.264	138	811.98	814.60
2	45.61	1.4163	1.285	140	897.4	894.19
3	59.44	1.5963	1.67	137	935.81	936.32

Table **3.1** shows the fission cross-section of $^1_0\text{n} \rightarrow ^{232}\text{Th} \rightarrow ^{233}\text{Th} \rightarrow A_1 + A_2$ reaction using DCM compared with the experimental data. One may clearly see that DCM based calculations find nice comparison with the experimental data with in one parameter (ΔR) fitting over a wide range of centre of mass energy. The neck length parameter increases almost linearly as a function of Ecm as depicted in Fig 3.8 .

Fig **3.1** shows the fragmentation potential for neutron induced fission of ^{232}Th nucleus at two extreme ℓ values, $\ell=0$ and $\ell=\ell_{\text{max}}$. The ℓ_{max} is taken in sticking moment of inertia approach and is decided where cross-section of light particles ($A_2 \leq 4$) become zero or alternatively when the penetrability becomes zero. One may clearly see that evaporation residue component is more prominent at $\ell=0$ values whereas fission starts competing at higher ℓ values. Although the behaviour of potential energy surfaces don't change much with angular momentum except for a point that fission distribution becomes more asymmetric at higher ℓ values as expected in case of neutron induced reactions.

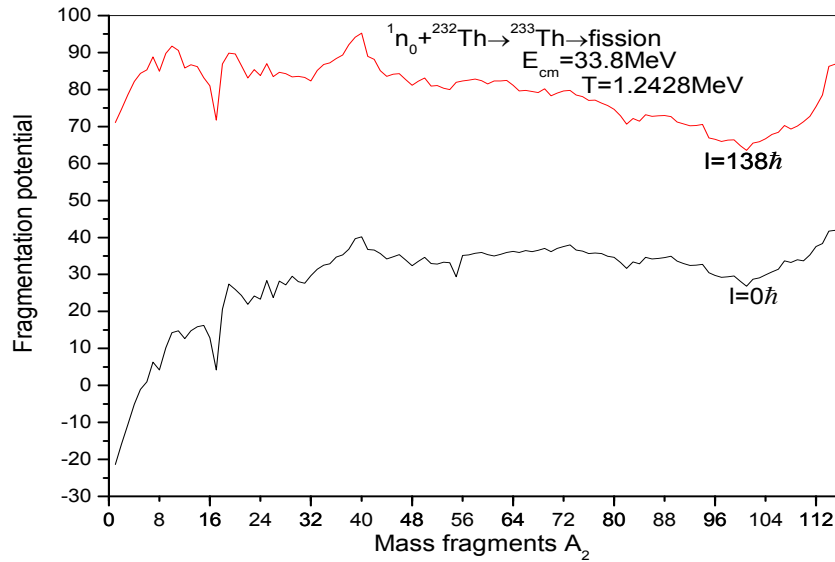


Fig:3.1 Fragmentation potential of ${}^1_0n + {}^{232}\text{Th} \rightarrow {}^{233}\text{Th} \rightarrow A_1 + A_2$ at $E_{\text{cm}}=33.8\text{MeV}$ at $\ell = 0$ and $\ell_{\text{max}}=138$.

Fig 3.2 shows the fragmentation potential of ${}^{232}\text{Th}$ formed in neutron induced reaction at $E_{\text{cm}}=33.8\text{MeV}$, 45.61MeV and 59.44MeV . Interestingly the potential energy surfaces remain almost identical with change in incident energy, without having difference in relative magnitude. Clearly the fission distribution remains asymmetric at all reported energies.

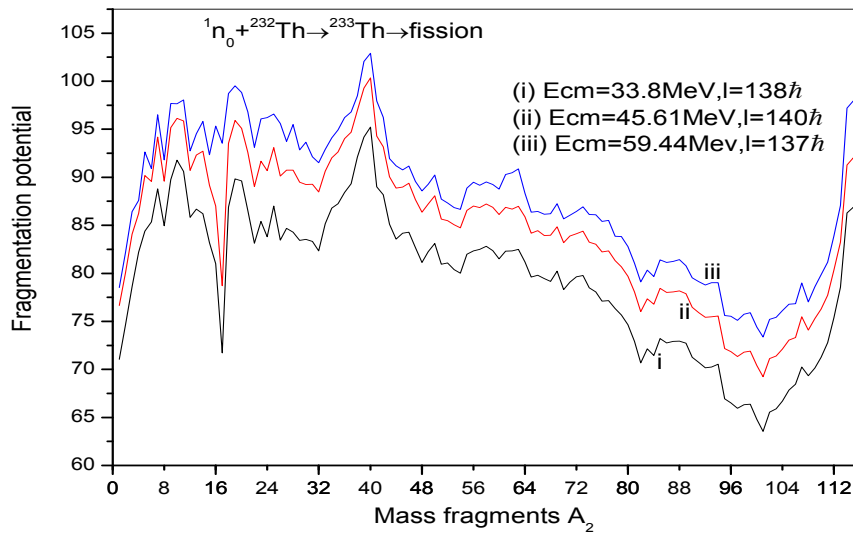


Fig:3.2 Fragmentation potential of ${}^1_0n + {}^{232}\text{Th} \rightarrow {}^{233}\text{Th} \rightarrow A_1 + A_2$ For $E_{\text{cm}} = 33.8\text{MeV}$, 45.61MeV , 59.44MeV at ℓ_{max} values

Fig.3.3 shows the preformation probability for $^1_0n + ^{232}_{90}\text{Th} \rightarrow ^{233}_{90}\text{Th} \rightarrow A_1 + A_2$ reaction at $E_{cm}=33.8\text{MeV}$ at two extreme values. It is important to note that the preformation probability (P_0) (also known as nuclear spectroscopy factor) imparts important nuclear structure information and is a very useful quantity in the framework of DCM. The fission distribution is asymmetric and the fragments in the range of 80-110 seem to be contributing towards fission yield.

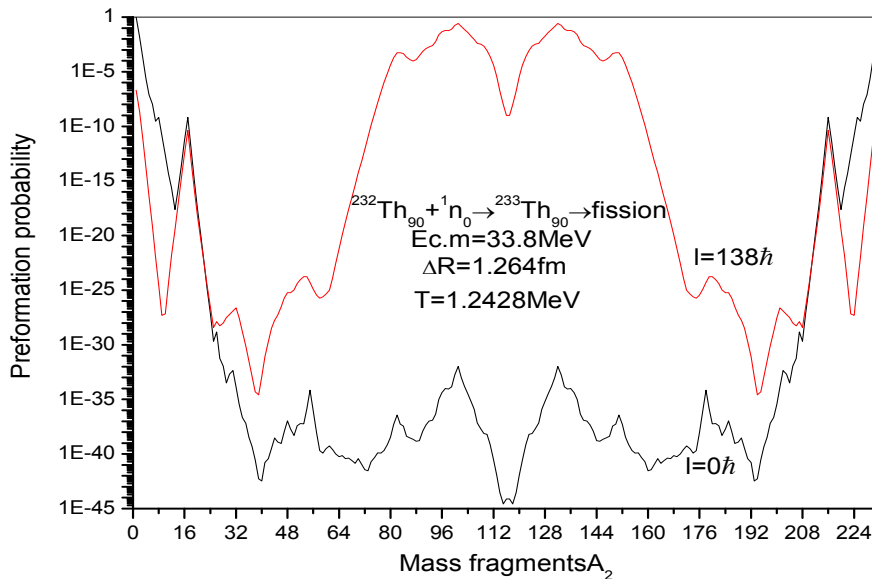


Fig:3.3 Preformation probability of fragments in fission of ^{233}Th in neutron induced reaction at $E_{cm}=33.8\text{MeV}$ by DCM

Fig 3.4 and 3.5 clearly show asymmetric fragmentation like in Fig3.3 and fragments in the range of $A_2 = 80-110$ seem to contribute at these higher energies as well. Although, the fragmentation path is asymmetric as shown that for Yukawa, Liquid drop and Yukawa+exponential distribution as reported in[10][11][12][13]. However the experimental observation indicate that fragmentation path become relatively more symmetric with increase in incident energy. Therefore one may conclude that although experimental fission cross-sections are fitted nicely within DCM, the observed change in fragmentation yield could not be achieved even with inclusion of deformation and orientation effects upto quadrupole deformations β_2 . It could be of further interest to look for the possible effect of higher

multipole deformations upto hexadecapole β_4 in order to check for the observed change in fission fragment distribution with increase in energy.

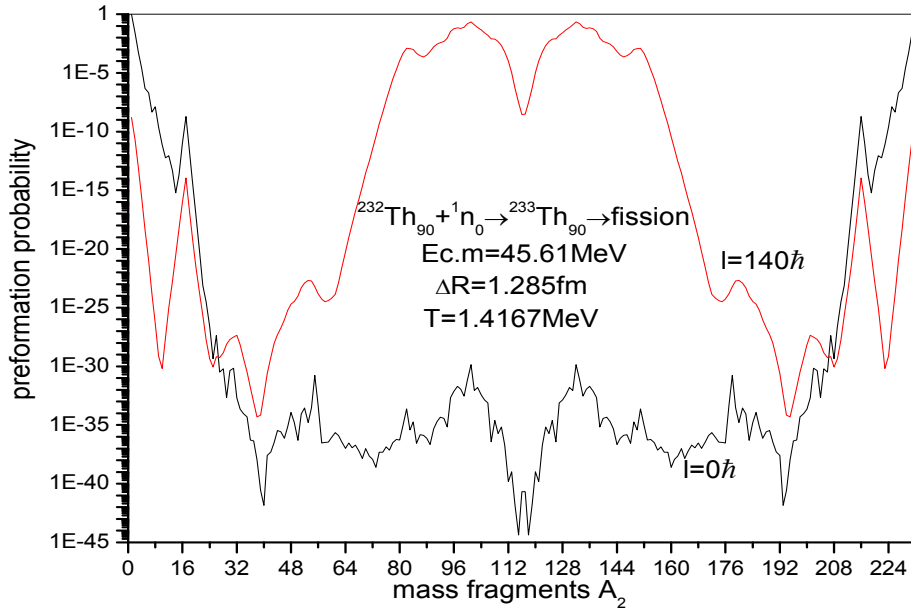


Fig:3.4 Preformation probability of fragments in fission of ^{233}Th in neutron induced reaction at $E_{cm}=45.61\text{MeV}$ by DCM

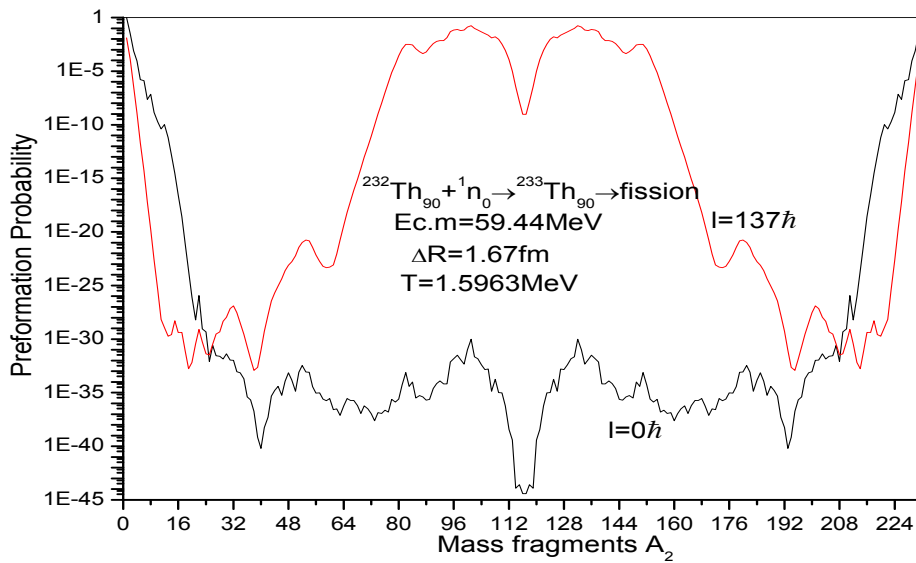


Fig:3.5 Preformation probability of fragments in fission of ^{233}Th in neutron induced reaction at $E_{cm}=59.44\text{MeV}$ by DCM

Fig 3.6 shows the penetrability as a function of fragment mass A_2 at $E_{cm}=33.8\text{MeV}$ at $\ell_{\max}=138$. The dip at ^{17}B may be due to some wrong estimation of quadrupole deformation. One may clearly see from this graph that there is hardly any structure in the penetrability value and it seem to contribute only towards the magnitude, which emphasize further that the nuclear structure information can be extracted only via preformation probability as stated in the discussion of figs: 3.3-3.5.

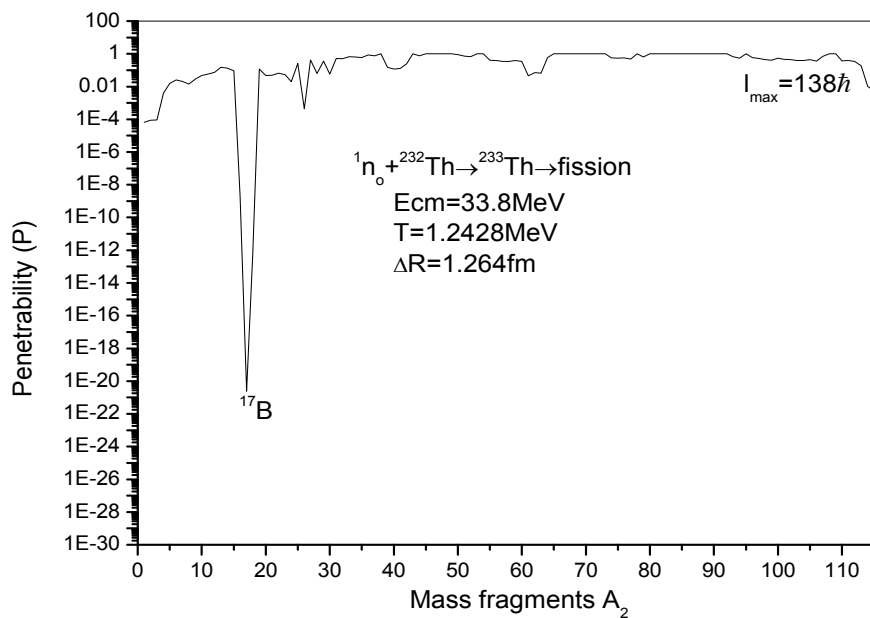


Fig3.6: Penetrability as a function of mass fragments A_2 at $E_{cm}=33.8\text{MeV}$

3.2 U-233(n,2n) CROSS-SECTIONS

After checking the status of DCM for neutron induced fission reaction, it has been further applied for (n,2n) reaction on ^{233}U nucleus. The Cascade 2004 code data [14,15] is available for (n,xn) reaction on ^{233}U nucleus, out of which (n,2n) data is tested in the framework of DCM over a wide range of incident energies. The DCM based (n,2n) cross-sections in energy range 25-100MeV find nice comparison in the reported data. The results are depicted in fig3.7 and table 3.2. Again DCM comparison is poor at energies $< 25\text{MeV}$ (not shown in fig.3.9) and further investigations are required in order to look out for the possible reason.

Table 3.2 DCM based (n,2n) cross-sections compared with Cascade 2004 Code

S.No.	Neutron energy (MeV)	Cascade2004 Cross-section (mb)	Cross-section By DCM (mb)	Neck Length Parameter (Fermi)
1	99.86	145.96	140.9	2.197
2	59.95	218.08	218.3	2.575
3	44.91	14.08	13.9	1.943
4	39.90	17.84	16.99	1.985
5	35.09	20.55	21.09	2.006
6	30.08	24.25	23.99	2.05
7	25.06	36.23	36.32	2.177

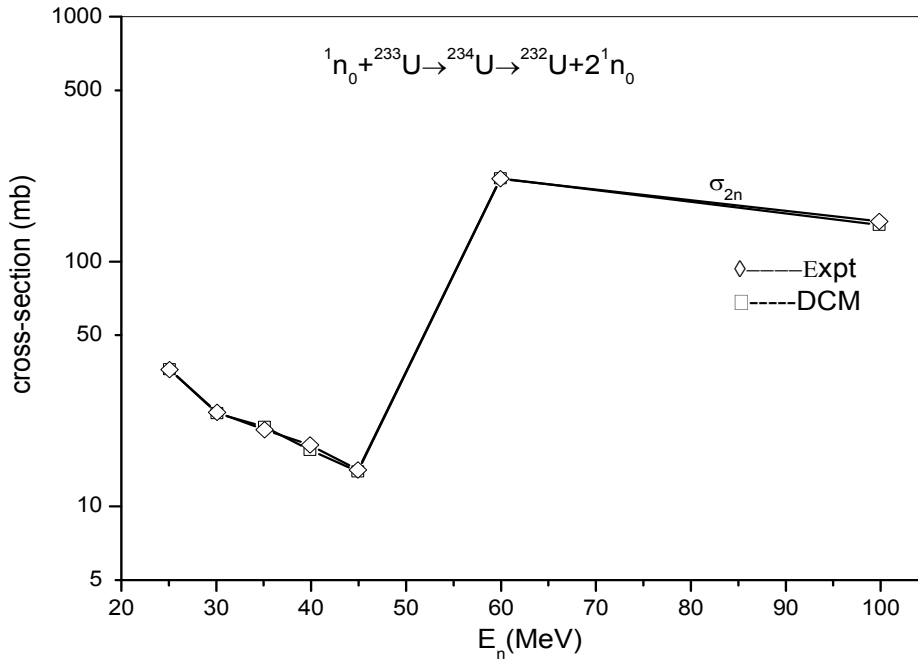


Fig 3.7: (n,2n) cross-sections of 233U nucleus

Fig 3.8 depicts the DCM based neutron induced fission cross-sections over a wide range of incident energies. The DCM based fission cross-sections find nice comparison with experimental data within one parameter i.e. neck length parameter (ΔR).

The neck length parameter increases as a function of incident energy as shown in fig.3.9 .

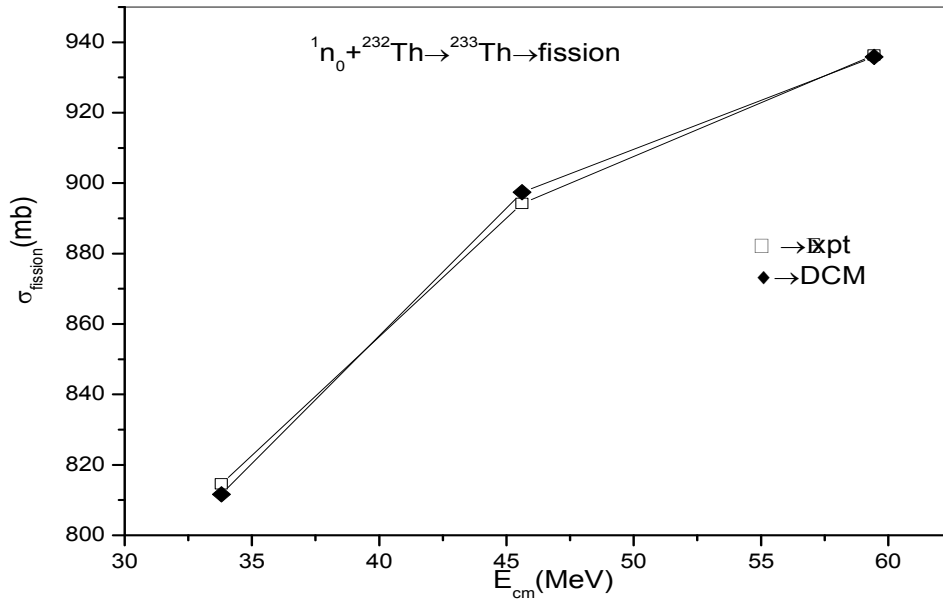


Fig 3.8 DCM based fission cross-sections compared with experiment

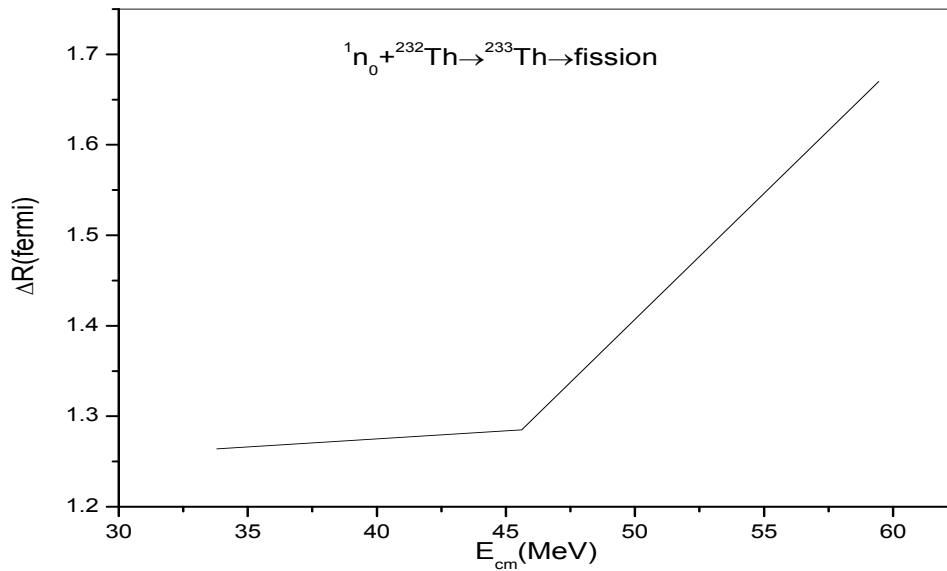


Fig 3.9 Neck length parameter as a function of E_{cm}

SUMMARY

In summary the Dynamical Cluster Decay Model(DCM) is applied for the first time in domain neutron induced reactions. The DCM based calculations for $^1_0n + ^{232}\text{Th} \rightarrow ^{233}\text{Th} \rightarrow \text{fission}$, find nice comparison with experimental data. Further the (n,2n) cross-sections of ^{233}U are also calculated using DCM, which find nice comparison with Cascade 2004 calculations. It will be of further interest to apply/modify the DCM in context of neutron induced reactions which find its applications in the nuclear energy sector.

3.3 REFERENCES

- [1.] M. Chadwick *et al.*, Nucl. Data Sheets **107**, 2931 (2006).
- [2] B. Wilkins, E. Steinberg, and R. Chasman, Phys. Rev. C **14**,1832 (1976).
- [3] J. Maruhn and W. Greiner, Phys. Rev. C **13**, 2404 (1975).
- [4] M. C. Duijvestijn, A. J. Koning, and F.-J. Hamsch, Phys. Rev.C **64**, 014607 (2001).
- [5] H. Goutte, J.-F. Berger, and D. Gogny, Int. J. Mod. Phys. E **15**,292 (2006).
- [6] S. Yavshits, in Proceedings of the Second International Workshop on Compound Nuclear Reactions and Related Topics CNR*09, Bordeaux, 2009 [EPJ Web Conf. **2**, 08004(2010)].
- [7] G. Audi and A.H. Wapstra and C. Thiboult, Nucl. Phys. A **729**, 337(2003)
- [8] P. Möller, J. R. Nix, W. D. Myers, and W. J. Swiatecki, At. Data Nucl. Data Tables **59**, 185 (1995).
- [9] V. Pronyaev *et al.*, in Proceedings of IAEA Co-ordinated Research Project on International Evaluation of Neutron Cross-Section Standards, STI/PUB/1291 (IAEA, Vienna, 2008),p. 122.
- [10] P. Seeger and W. Howard, At. Data Nucl. Data Tables **17**, 428(1976).
- [11] H. Krappe and J. Nix, in Proceedings of the Third International Symposium on Physics and Chemistry of Fission, Rochester, 1973 (IAEA, Vienna, 1974), Vol. 1,p. 159.
- [12] A. Dobrowolski, K. Pomorski, and J. Bartel, Phys. Rev. C **75**,024613 (2007); Phys. Scr., T **125**, 188 (2006).
- [13] H. J. Krappe, J. R. Nix, and A. J. Sierk, Phys. Rev. C **20**, 992(1979).
- [14.] V S Barashenkov and H Kumawat, Development of Monte Carlo model of high-energy nuclear interactions, JINR E11-2004-121, Dubna, 2004
- [15.] H Kumawat and V S Barashenkov, *Euro. Phys. J. A* (submitted)